Liquid biopsy of cerebrospinal fluid enables selective profiling of glioma molecular subtypes at first clinical presentation

Francesca Orzan[1§], Francesca De Bacco[1,2§], Elisabetta Lazzarini[3§], Giovanni Crisafulli[4], Alessandra Gasparini[3], Angelo Dipasquale[5,6], Ludovic Barault[7,2], Marco Macagno[7], Pasquale Persico[5,6], Federico Pessina[5,6], Beatrice Bono[5], Laura Giordano[5], Pietro Zeppa[8], Antonio Melcarne[9], Paola Cassoni[10], Diego Garbossa[8], Armando Santoro[5,6], Paolo M. Comoglio[4], Stefano Indraccolo[3,11], Matteo Simonelli[5,6,#] and Carla Boccaccio[1,2,#*]

[1]Laboratory of Cancer Stem Cell Research, Candiolo Cancer Institute, FPO-IRCCS, 10060 Candiolo, Turin, Italy

[2] Department of Oncology, University of Turin Medical School, 10060 Candiolo, Turin, Italy

[3]Basic and Translational Oncology Unit, Veneto Institute of Oncology IOV-IRCCS, 35128 Padua, Italy

[4] IFOM ETS – The AIRC Institute of Molecular Oncology, 20139 Milan, Italy

[5] IRCCS Humanitas Research Hospital, 20089 Rozzano (Milan), Italy

[6]Department of Biomedical Sciences, Humanitas University, 20090 Pieve Emanuele (Milan), Italy

[7]Laboratory of Cancer Epigenetics, Candiolo Cancer Institute, FPO-IRCCS, 10060 Candiolo, Turin, Italy

[8]Department of Neurosciences, University of Turin Medical School, 10126 Turin, Italy

[9] Città della Salute e della Scienza, 10126 Turin, Italy

[10] Department of Medical Sciences, University of Turin Medical School, 10126 Turin, Italy

[11]Department of Surgery, Oncology and Gastroenterology, University of Padova, 35123 Padua, Italy

§Equal contribution

#Equal contribution

**Corresponding author:* Carla Boccaccio, Candiolo Cancer Institute, FPO-IRCCS, Str. Prov. 142, Km. 3.95, 10060 Candiolo, Turin, Italy. Phone: +39-011-9933208. E-mail: carla.boccaccio@ircc.it.

Running title. Liquid biopsy of cerebrospinal fluid for glioma diagnosis

Keywords. Liquid biopsy, cerebrospinal fluid, glioma, glioblastoma, circulating tumor DNA, cell free DNA, NGS, ddPCR, *MGMT*, p*TERT*, *IDH*.

CONFLICT OF INTEREST

All authors declare that they have no competing interests.

ABSTRACT

Purpose: Current glioma diagnostic guidelines call for molecular profiling to stratify patients into prognostic and treatment subgroups. In case the tumor tissue is inaccessible, cerebrospinal fluid (CSF) has been proposed as a reliable tumor DNA source for liquid biopsy. We prospectively investigated the use of CSF for molecular characterization of newly diagnosed gliomas.

Experimental design: We recruited two cohorts of newly diagnosed glioma patients, one (n=45) providing CSF collected in proximity of the tumor, the other (n=39) CSF collected by lumbar puncture. Both cohorts provided tumor tissues by surgery concomitant with CSF sampling. DNA samples retrieved from CSF and matched tumors were systematically characterized and compared by comprehensive (NGS) or targeted (ddPCR) methodologies. Conventional and molecular diagnosis outcomes were compared.

Results: We report that tumor DNA is abundant in CSF close to the tumor, but scanty and mostly below NGS sensitivity threshold in CSF from lumbar puncture. Indeed, tumor DNA is mostly released by cells invading liquoral spaces, generating a gradient that attenuates by departing from the tumor. Nevertheless, in >60% of lumbar puncture CSF samples, tumor DNA is sufficient to assess a selected panel of genetic alterations (*IDH* and *TERT* promoter mutations, *EGFR* amplification, *CDKN2A/B* deletion: ITEC protocol) and *MGMT* methylation that, combined with imaging, enable tissue-agnostic identification of main glioma molecular subtypes.

Conclusions: This study shows potentialities and limitations of CSF liquid biopsy in achieving molecular characterization of gliomas at first clinical presentation and proposes a protocol to maximize diagnostic information retrievable from CSF DNA.

TRANSLATIONAL RELEVANCE

In primary brain tumors, the presence of the blood-brain-barrier hampers the release of significant tumor DNA into the circulation, limiting the feasibility of blood-based liquid biopsy strategies. The possibility to exploit CSF (cerebrospinal fluid) as an alternative source of circulating tumor DNA for broad genetic profiling of gliomas is currently under investigation. This is the first study that prospectively explores the use of CSF-based liquid biopsy for molecular characterization of newly diagnosed malignant gliomas. Here we show that the yield of tumor DNA in CSF from lumbar puncture is very poor, preventing the application of a comprehensive NGS analysis in most cases. Nevertheless, we demonstrate the systematic feasibility of a high-sensitivity ddPCR-based protocol (ITEC) covering a set of glioma specific genetic alterations with diagnostic and predictive significance. This tool may be applied when the tumor is not surgically approachable, allowing a presumptive molecular diagnosis according to WHO2021 criteria and a tailored treatment.

INTRODUCTION

The 2021 WHO classification of brain tumors emphasizes the primacy of molecular characterization for glioma subtyping (1, 2). Accordingly, on the one hand, detection of an isocitrate dehydrogenase (*IDH*) wild-type gene is required to classify a glioma as a glioblastoma (GBM); on the other hand, the presence of a limited set of genetic features, such as *IDH*-wild type gene together with either telomerase reverse transcriptase promoter (p*TERT*) mutation, or epidermal growth factor receptor (*EGFR*) gene amplification, or gain of entire chromosome 7 combined with loss of chromosome 10, is sufficient to classify a glioma as a GBM even in the absence of distinctive GBM histopathological features (1-3). Among *IDH*-mutant gliomas, grading takes into account the presence of cyclin dependent kinase inhibitor 2A/B (*CDKN2A/B*) homozygous deletion, which defines grade 4 and results in worse prognosis regardless of histopathology. Characterization of such genetic biomarkers has therefore diagnostic and prognostic implications and requires to be implemented in the routine clinical setting. Besides, although the number of recognized biomarkers is currently limited, the increased cost-effectiveness of NGS technologies offers the opportunity to replace targeted with comprehensive sequential analyses (4).

In gliomas, standard molecular characterization based on tumor tissue samples can occasionally be unfeasible, due to inaccessible tumor location, or it can suffer from several limitations, including failure to recapitulate the well-known intratumor glioma genetic heterogeneity (5) and to detect genetic alterations (in particular gene copy number loss) for excessive contamination by non-tumor tissue. Moreover, if longitudinal patient monitoring is needed, repeated biopsies can be hard to obtain, precluding a new molecular characterization of recurrent tumors.

In recent years, liquid biopsy of cell-free circulating tumor DNA (cfDNA) has emerged as an intriguing alternative to tissue biopsy. Beside portability, liquid biopsy offers better chances to capture tumor genetic heterogeneity and to assist in longitudinal monitoring of the patient, being in principle able to provide information on tumor genetic evolution over time, and on the ensuing emergence of predictive or response biomarkers (6-8). This is critical to select patients for targeted therapies that recently yielded encouraging results (9-12). Moreover, liquid biopsy could help to measure tumor burden in response to treatments, as MRI-based neuroimaging can fail to identify pseudoprogression and pseudoresponse (13).

Unlike in other tumors, blood was shown to be a poor source of brain tumor cfDNA (14-16). Conversely, cerebrospinal fluid (CSF) seems to offer the opportunity to retrieve tumor DNA and to analyze genetic alterations either by targeted or more comprehensive NGS methodologies in both adult and pediatric gliomas and medulloblastomas (15-23). However, substantial questions await to be solved for translating CSF liquid biopsy into clinical practice and to align liquid biopsy purposes with our current understanding of glioma genetics and its impact on clinical management.

In particular, we still need prospective studies that systematically address: (i) the possibility of finding tumor DNA in CSF collected by lumbar puncture (LP-CSF) in glioma patients at first diagnosis, before surgery and radiotherapy; (ii) the qualitative and quantitative features of CSF tumor DNA, which depend on the still unclear sources of the DNA and its circulation dynamics in CSF, and strongly influence the possibility of detection by current techniques; (iii) whether performing an extensive NGS analysis of CSF tumor DNA is feasible in newly diagnosed, presurgical patients; (iv) how closely the genetic alterations found in LP-CSF recapitulate those found in matched tumor tissues.

To answer these questions, in this work we analyzed two cohorts of gliomas at first diagnosis, one providing peritumoral CSF, the other LP-CSF, and both giving tumor tissues by surgery concomitant with CSF sampling.

MATERIALS AND METHODS

Human subjects

Cohort 1 patients with a diagnosis of primary brain tumors according to WHO guidelines were enrolled and treated at the "Città della Salute e della Scienza" (University of Torino, Italy) in a prospective observational trial (ClinicalTrials.gov, https://clinicaltrials.gov/ct2/show/NCT03347318?term=001-IRCC-00IIS-10&draw=2&rank=1, N° NCT03347318) approved by the Ethical Committee of Città della Salute e della Scienza (Torino, Italy). In Cohort 2 patients with a diagnosis of primary brain tumor according to WHO guidelines were enrolled and treated at "IRCCS, Humanitas Research Hospital" (Humanitas University, Italy) in a prospective observational trial (ONC/OSS-06/2017) approved by the Ethical Committee of IRCCS, Humanitas Research Hospital (Rozzano, Milan, Italy). For both cohorts informed written consent stating that the samples collected could be used for research was obtained from all patients and the study was conducted in accordance with the Declaration of Helsinki. All patient data and samples were de-identified before processing.

Analysis of imaging data

Pre-operative brain magnetic resonance imaging (Brain MRI) scans performed just before CSF sampling and including at least T1 pre- and post-contrast enhancement, T2, fluid-attenuated inversion recovery (FLAIR) and diffusion weighted sequences, were collected and analyzed to describe tumor characteristics in a blinded manner to information about DNA concentration. The area of tumor was measured using the maximal diameter (D) and a second perpendicular measurement (d) on the axial slides of T1 post-contrast enhancement or FLAIR sequences, according to the presence or absence of contrast-enhancement respectively. The lesion was

defined as abutting the CSF space if in contact with at least one of the primary liquor reservoirs such as ventricles or basal and other cisterns. Tumor disease progression was established according to Radiological Assessment in Neuro-oncology (RANO) criteria or after a multidisciplinary tumor board discussion.

Sample collection and preprocessing

In Cohort 1 patients, peritumoral CSF samples were collected at the opening of the surgical field, in proximity of the tumor and before tumor removal, by leakage from the subarachnoid space (n = 43) or by aspiration from the ventricle (n = 2). In all Cohort 2 patients, CSF was collected by lumbar puncture (LP), in 38/39 patients prior to surgery and, in one patient (MG2046), 2 months after the primary diagnosis to relieve obstructive hydrocephalus. In one patient (MG2049), CSF was collected twice, before first and second surgery for tumor recurrence, so that Cohort 2 provided a total of 40 LP-CSF samples. In both Cohort, after collection, CSFs were immediately centrifuged at 2000 rpm for 10' at room temperature (RT) according to previous protocols (16, 17, 23) and the presence of blood traces was annotated. Supernatants were carefully recovered for cfDNA isolation, further centrifuged at 4000 rpm for 10 minutes and immediately stored at -80°C. In Cohort 2, after the first centrifugation, pellets were recovered for cellular DNA isolation, and stored at -80°C. From each patient, at least 5 ml of whole blood was collected in Na_2EDTA coated tubes and centrifuged at 2000 rpm for 10' RT. Then, plasma was recovered, centrifuged at 4000 rpm for 10' RT and stored at -80°C. The remaining cellular fraction underwent erythrocyte lysis using 10 vol/vol ACK lysis solution (0.15M NH_4Cl, 1mM $KHCO_3$, 0.1mM Na_2EDTA, pH 7.4) and centrifugation at 1200 rpm for 5'. The pellet (containing

leukocytes) was resuspended in PBS and stored at -80°C. Fresh tumor tissues were collected during surgery and stored -80°C, or formalin fixed and paraffin embedded.

DNA extraction, quantitative and qualitative analysis

DNA extraction was centralized for all samples. DNA from CSF supernatant was extracted using QIAamp® MinElute® ccfDNA Mini Kit (Qiagen); DNA from fresh tumor tissues, blood leukocytes and CSF pellet was extracted using ReliaPrep™ gDNA Tissue Miniprep System (Promega); DNA from FFPE tumor tissue samples was extracted using Maxwell® RSC DNA FFPE Kit (Promega). DNA from CSF supernatant and pellet was quantified using Qubit™ dsDNA HS Assay Kit (ThermoFisher) and qualitative fragmentation analysis was performed using Agilent High Sensitivity DNA Kit and 2100 Bioanalyzer Instrument (Agilent). DNA from tumor tissues and blood leukocytes were analyzed with DS-11 FX Series Spectrophotometer/Fluorometer (DeNovix) and quantified using Qubit™ dsDNA HS/BR Assay Kits (ThermoFisher). All procedures related to DNA extraction and analysis were performed according to manufacturer's instructions.

Sanger Sequencing (Cohort 1 and 2 tumors)

In tumor gDNA samples (Cohort 1), *IDH1/2* and p*TERT* hotspot mutations, and *TP53* and phosphatase and tensin homolog (*PTEN*) full-length sequences were analyzed by Sanger Sequencing as detailed in Supplementary Information. In Cohort 2, p*TERT* hotspot mutations were analyzed by Sanger Sequencing as well. Data were processed by Chromas Lite 2.01 software (http://www.technelysium.com.au/chromas_lite.html) and compared with reference sequences from the Homo sapiens assembly GRCh37. All identified variants were analyzed for

possible pathogenicity using MutationTaster2021 (24) and compared with those in the Catalogue Of Somatic Mutations In Cancer (COSMIC, https://cancer.sanger.ac.uk/cosmic) and in IARC *TP53* DATABASE (https://tp53.isb-cgc.org/) (25).

Evaluation of *IDH1* and *2* mutations (Cohort 2 tumors)

IDH1 and *2* mutations targeted to specific codons (R132 in *IDH1* and R172 in *IDH*2) were tested by pyrosequencing using *IDH1*/2 status kit (Diatech Pharmacogenetics) according to manufacturer's instructions. *IDH1* R132H mutation was revealed also by immunohistochemistry using anti-*IDH1* R132H mouse monoclonal antibody (Clone H09; Dianova GmbH) on Benchmark Instrument (Ventana).

Gene copy number variation (CNV) analysis by qPCR (Cohort 1 tumors)

Gene CNV analysis was performed by real-time PCR, using TaqMan™ Universal PCR Master Mix and the ABI PRISM 7900HT sequence detection system (Thermo Fisher). TaqMan copy number assays are listed in Supplementary Information (Key Resource Table) and Supplementary Data 1. Relative gene CNV were calculated by normalizing vs. multiple endogenous controls (*GREB1*, *TERT*, *APOA1*, *RNaseP*; results are reported vs. *RNAseP*). For *CDKN2A/B* locus, a *CDKN2A* specific probe was used. A normal diploid human gDNA was used as calibrator to obtain the ΔΔCt. The copy number of each gene was calculated with the formula $2x2^{-\Delta\Delta Ct}$. Aberrant CNVs have been defined as follows: amplifications, CN > 5; deletions, CN < 1.5; gains, 3 > CN > 5.

EGFR CNV by FISH analysis (Cohort 2 tumors)

Fluorescence in situ hybridization (FISH) was performed on 4 μm paraffin sections using the Tissue Digestion Kit (Kreatech Biotechnology) according to manufacturer's instructions. The analyses were performed using *EGFR*/CEN7 dual-color probes (ZytoVision GmbH). Labeled SPEC *EGFR* probe is specific for the *EGFR* gene at 7p11.2. 100 tumor cell nuclei were scored in 3 different fields. *EGFR* is considered amplified if *EGFR*/CEN7 ratio is > 2 or if *EGFR* green signal clusters are observed.

droplet digital PCR (ddPCR; Cohort 1 and 2, tumors and CSF)

ddPCR was performed using probe–based assays with ddPCR Supermix for Probes (no dUTP) (Biorad) following manufacturers' instructions. Droplets were generated using AutoDG Droplet Digital PCR System (Biorad) and analyzed on a QX200 Droplet Digital PCR System using QX Manager Software Standard Edition, Version 1.2 (Biorad). *CDKN2A*, cyclin dependent kinase 4 (*CDK4*) and platelet derived growth factor receptor A (*PDGFRA*) CNV were normalized vs. *EIF2C1*, *RPP30* and *AP3B1*. *EGFR* CNV was normalized vs. *EIF2C1*, *RPP30* and *AP3B1* or vs. *VOPP1* and *ASL* (mapping near chr 7 centromere), as to distinguish real CNV from chr 7 polysomy. *IDH1*, *TP53* and *PTEN* mutations were analyzed following manufacturer's instructions. p*TERT* analysis was performed according to (26). For all assays, the minimum number of PCR-positive droplets (n = 30) was calculated according to (27). The presence of mutations was confirmed when 3/30 droplets amplified the mutation. Specific ddPCR assays are reported in Supplementary Information (Key Resource Table). Aberrant CNVs were defined as follows: amplifications, CN > 5; deletions, CN < 1.5; gains, 3 > CN > 5.

NGS analysis by a targeted panel (Cohort 1 and 2, tumors and CSF)

We designed a 388,773kb capture-based custom panel including all coding regions of 54 glioma-associated genes (see Supplementary Data 2). Libraries were constructed starting from >10 ng DNA using the "SureSelectXT HS Target Enrichment System for Illumina Paired-End Multiplexed Sequencing Library" kit (Agilent Technologies, Santa Clara, USA), according to manufacturer's instructions. Libraries were sequenced on MiSeq sequencer (Illumina, San Diego, USA) with 150 bps paired-end reads. NGS data were processed both using a custom analysis pipeline developed in collaboration with OncoDNA (www.oncodna.com) (28) using SureCall software as caller (version 4.1.1.5, Agilent Technologies, Santa Clara, CA) and the bioinformatic pipeline previously described in (29, 30). A metanormal was built from fastq files obtained by 10 PBMC samples sequenced as previously described (31).To delete NGS artifacts, mutations were further filtered as previously described (30, 31). Indels were called using Pindel tool in both alignments and only somatic indels with fractional abundance > 10% were reported. Gene copy number variations analysis was performed in the matched samples (tumor/liquor/pellet vs. metanormal) for each patient. Gene copy number (CN) was calculated as the ratio of median gene depth and the median depth of all genomic regions covered in the panel. For each gene, the copy number variation (CNV) was calculated as the ratio between CN of metanormal sample and CN of the same gene in the tumor/liquor/pellet one as previously reported (29-31). Sample authentication was performed using the list of "panel-covered" single-nucleotide polymorphisms (SNPs) listed in dbSNP version 147. An allele was considered only if the fractional abundance was higher than 30% with a minimum depth of 20X (31). All SNP_ID were compared to establish the correct sample matching. All identified variants were analyzed for possible pathogenicity as above. Amplifications and deletions were considered significant in

oncogenes and tumor suppressor genes, respectively, based on annotation in OncoKB (https://www.oncokb.org/) (32).

Analysis of *MGMT* promoter methylation (Cohort 1 and 2, tumors and CSF)

Bisulfite conversion of DNA extracted from tumors or CSF was performed by EZ DNA methylation Gold kit (Zymo Research). In Cohort 1 tumors and CSF, and in Cohort 2 CSF, *MGMT* (O-6-methylguanine-DNA methyltransferase) promoter methylation was assessed by methyl-BEAMing multistep digital PCR according to (33). In Cohort 2 tumors, it was assessed by pyrosequencing. For details see Supplementary Information.

Statistical analysis

When appropriate, descriptive statistical data were reported (median, confidence interval). Statistical comparisons were performed using the non-parametric Spearman's rank correlation. Where indicated, Fisher exact test with Bonferroni correction or Chi-square test were applied. Data were summarized as frequencies and proportions or as medians and range, as appropriate. For continuous data, the Wilcoxon (Mann-Whitney) *t test* was used to compare differences between groups and the Pearson correlation coefficient to evaluate linear correlation. Progression-free survival and overall survival were estimated using Kaplan-Meier curves. All the reported p-values were two-sided. A p-value <0.05 was considered significant. Analyses were performed using Statistical Analysis System (SAS) version 9.4 or Prism v8.0 software (GraphPad).

Data Availability

Complete datasets related to NGS analysis (referring to Fig. 2I, 3G, Supplementary Fig. S3, and Supplementary Tables S5 and S10) are available as Supplementary Data 2 (sheets 1-3). Raw NGS data are available at the European Nucleotide Archive under project accession number PRJEB55332, study ERP140225 (https://www.ebi.ac.uk/ena/browser/search). All other data supporting the findings of this study are available within the article, Supplementary Information and Supplementary Data 1 and 3. Other related data are available from the corresponding author upon reasonable request.

RESULTS

A glioma cohort for comparative analysis of peritumoral CSF and tumor tissue

To systematically investigate the feasibility of CSF liquid biopsy by NGS in newly diagnosed glioma patients, we collected a cohort of 45 patients with presumptive primary GBM at the time of surgery (Cohort 1, Supplementary Table S1). From each patient, we retrieved a tumor tissue sample, a peritumoral CSF sample (cell-free supernatant) from brain liquoral spaces in proximity with the surgical field, and a blood sample, with the aim to assess whether the main genetic alterations found in tumor tissues could be detected in the matched CSF and blood plasma as well (Fig. 1A). DNA from each tissue sample (n = 45) was analyzed with Sanger sequencing or qPCR to investigate *IDH1/2* status and the presence of additional alterations relevant for molecular characterization (*TERT* promoter mutation, *EGFR* amplification, and *CDKN2A/B* deep deletion) (1, 2), or known to recur in at least 15% of the GBM population (*PTEN* and *TP53* mutation, and *PDGFRA* and *CDK4* amplification). After this analysis, 40/45 tumor tissues displayed at least one genetic alteration to be searched in CSF and plasma (Fig. 1A and B and Supplementary Table S2).

Comparative targeted genetic analysis of peritumoral CSF and tumor tissues

Peritumoral CSF samples underwent quantitative cfDNA analysis, showing that the majority of samples (38/45) contained 10-200 ng of DNA, while the remaining 7/45 samples did not contain detectable DNA (median concentration of all samples: 77.2 ng/ml; Fig. 2A and B and Supplementary Table S3). A weak positive correlation between the CSF volume and its total cfDNA amount was found (r = 0.36, p = 0.014, Fig. 2A). The median CSF cfDNA concentration was higher in tumors defined as abutting the liquoral spaces vs. those that were not, and in grade 4 tumors vs. grade 1-3, although without reaching statistical significance. No correlation was

observed between cfDNA concentration on the one hand and tumor size on the other (Fig. 2C, Supplementary Tables S1 and S3).

cfDNA qualitative analysis to determine DNA molecular weight (MW) showed that 6/45 samples contained only low-MW DNA, 16/45 contained only high-MW DNA and 8/45 contained both low- and high-MW DNA; in the remaining 15/45 samples, the DNA MW profile could not be analyzed for technical reasons (Fig. 2D and Supplementary Table S3). In CSF from brain tumor patients, the presence of low-MW DNA, derived from apoptotic tumor DNA fragmentation and supposed to be released in CSF by ultrafiltration, is expected (34). The unforeseen presence of poorly soluble high-MW DNA in 24/45 samples suggested that this DNA could derive from tumor cells that had accumulated in peritumoral CSF spaces. This conclusion was supported by experiments showing that GBM primary cells (neurospheres derived from Cohort 1 patients CT025 and CT151), after incubation in artificial CSF, could survive for days and then release high-MW DNA, likely after necrosis (Supplementary Fig. S1A-C).

Next, to verify whether CSF cfDNA contained circulating tumor DNA, genetic alterations found in tumor tissues were searched in the corresponding CSFs by highly sensitive and specific ddPCR assays (n = 40, including those where DNA could not be quantified) (Fig. 2E and F and Supplementary Table S4). Excluding a fraction of CSF cfDNAs that failed to provide a positive control for ddPCR amplification (n = 4/40), in the remaining cases at least one genetic alteration, either a copy number variation (CNV), or gene mutation, could be found in 25/36 CSFs (Fig. 2E and F and Supplementary Table S4). A high amount of cfDNA was associated with high probability to detect circulating tumor DNA (Chi-square for a trend, P = 0.0096, df = 1), but it was not an absolute requirement. Indeed, 14/15 CSFs with high cfDNA concentration (> 200 ng/ml) displayed the tumor alteration, while CSFs displaying a cfDNA

concentration of 10-200 ng/ml, which represented the majority of cases, included cases that either displayed (n = 8/20) or not (n = 12/20) the tumor genetic alteration. Importantly, even 3/6 CSF samples with very low cfDNA concentration (< 10 ng/ml) displayed the tumor mutation, attesting the extreme sensitivity of the ddPCR technique (Fig. 2G). Mutations were detected not only in low-MW but also in high-MW DNA, in comparable sample fractions (Fig. 2G), indicating that tumor cells invading CSF spaces may be a relevant source of cfDNA.

Blood plasma is known to rarely contain cfDNA released by adult gliomas (14). In line with previous observations, in 7/7 blood plasma analyzed we could not detect the genetic alterations present in tissues and CSFs (Fig. 2E and F and Supplementary Table S4), leading to discontinue plasma analysis.

In summary, in Cohort 1, 40/45 patients displayed, in their tumor tissues, at least one mutation suitable to the design of a ddPCR assay. Of these patients, 36/40 yielded peritumoral CSFs containing cfDNA that could be amplified for ddPCR and undergo assessment of the tumor genetic alteration. In 25/36 cfDNAs assessed by ddPCR, the tumor genetic alteration was detected, indicating the unequivocal presence of circulating tumor DNA in CSF. Of these 25 CSF samples, 22 provided the minimal DNA amount required for NGS (> 10 ng) (Fig. 2H). Within this group, 3 cases, including CSF samples representative of either low-, high- or mixed DNA MW (Supplementary Table S3), were chosen to undergo the NGS analysis.

Comparative NGS analysis of peritumoral CSF and tumor DNA

NGS analysis of peritumoral CSF and matched tumor tissue DNA (n = 3 pairs) was performed by using a panel including 54 glioma-related genes (Supplementary Data 2). In both tissues and CSFs, NGS analysis confirmed the presence of the genetic alterations revealed by targeted

analysis and detected additional alterations, identical in paired tissues and CSFs, with the exception of a phosphoinositide-3-kinase regulatory subunit 1 (*PIK3R1*) mutation, which was found at low frequency only in patient CT116 cfDNA. Moreover, NGS showed that VAFs and CNVs were increased in CSF cfDNAs compared with matched tissue DNAs, indicating that, at least in this sample panel, CSF was relatively enriched in tumor DNA (Fig. 2I, Supplementary Table S5 and Supplementary Data 2).

A prospective glioma cohort for analysis of CSF DNA retrieved by lumbar puncture

The results of tumor and peritumoral CSF comparative analysis encouraged to explore the possibility to apply NGS to CSF collected by lumbar puncture (hereafter indicated as LP-CSF), in view of potential application in daily clinical practice for glioma patients ineligible to surgery, or for a longitudinal genomic monitoring over the course of treatments. As systematic information on LP-CSF reliability for NGS analysis of newly diagnosed gliomas is missing (6, 7), we collected a prospective cohort of 39 patients with suspected gliomas based on radiologic criteria, and eligible to surgery (Cohort 2, Fig. 3A and Supplementary Table S6). Cohort 2 provided 33 primary, 5 recurrent, and a pair of primary and recurrent tumors from the same patient (MG2049), for a total of 40 tumor samples (Fig. 3A). LP-CSFs were mostly collected immediately prior to surgery (n = 39) or, in one case, 2 months after the first surgery, during LP to relieve hydrocephalus, for a total of 40 LP-CSFs (Fig. 3A and Supplementary Table S6). Considering that analysis of peritumoral cfDNA showed the frequent presence of high-MW DNA (Fig. 2D and G), which is likely released from cells invading CSF spaces, and that glioma cells can survive longtime in the CSF milieu (Supplementary Fig. S1A and B), in most cases (n = 37) we extracted DNA not only from CSF supernatants (cfDNA), but also from intact cells contained in CSF pellets (cellular DNA) (Fig. 3A). CSF supernatants were expected to contain

both low- and high-MW DNA, while CSF pellets were expected to contain mostly high-MW DNA.

After surgery, tumor tissues underwent routine histopathological diagnosis and analysis of *IDH1/2* mutation, *pTERT* and *EGFR* amplification, leading to diagnose 31 GBM *IDH* wild-type (*IDH*-wt), 4 *IDH*-mutant (*IDH*-mut) astrocytomas, 2 *IDH*-mut oligodendrogliomas, one ependymoma and one ganglioglioma (Fig. 3B and Supplementary Tables S6 and S7). Ependymoma and ganglioglioma were excluded from the study as they are rare entities, not classified as adult-type diffuse gliomas, and displaying a distinct molecular profile. Tumor tissues were further exploited to validate NGS analysis of LP-CSF (Fig. 3A).

In Cohort 2, LP-CSF displayed a modest median DNA concentration of 0.05 ng/ml in the supernatant and 2.14 ng/ml in the pellet (Fig. 3C and Supplementary Table S8), remarkably lower than the median cfDNA concentration (77.2 ng/ml) found in peritumoral CSFs (Cohort 1, Fig. 2B). Like in Cohort 1, a weak positive correlation between the LP-CSF volume and its DNA content was found (Fig. 3D; correlation between cfDNA amount and LP-CSF volume, $r = 0.38$, $p = 0.021$; between cellular DNA and LP-CSF volume, $r = 0.10$, $p = 0.56$). Interestingly, the median cfDNA concentration in LP-CSF from newly diagnosed tumors was lower than in recurrent tumors, without reaching statistical significance (0.04 ng/ml vs. 0.81 ng/ml, Mann-Whitney test, $p = 0.13$, Supplementary Table S8). DNA qualitative analysis of LP-CSF supernatants (feasible only in 8/40 samples) showed that 5/8 samples contained only low-MW DNA, 2/8 mixed-MW DNA and 1/8 only high-MW DNA. As expected, cellular DNA was invariably high-MW (Supplementary Table S8).

As previously reported (15), in Cohort 2, a significant correlation was found between median LP-CSF cfDNA concentration and tumor proximity with liquoral spaces, again

supporting the notion that CSF cfDNA mostly derives from cells invading such spaces (Fig. 3E and Supplementary Table S9). No correlation was found between LP-CSF cfDNA concentration and tumor grade, or tumor size (tumor maximal diameter or tumor area) (Fig. 3E), or tumor progression (Supplementary Fig. S2A and B).

Overall, in Cohort 2 patients, the minimal absolute DNA quantity required for NGS (10 ng) was reached in only 5/38 cfDNA samples from supernatants and in 14/35 cellular DNA samples from pellets, for a total of 19/73 samples. These samples corresponded to 16/37 patients, including 10/31 primary and 6/6 recurrent gliomas (Fig. 3D and F and Supplementary Table S8).

Comparative NGS analysis of LP-CSF and tumor DNA

Eleven LP-CSF samples containing at least 10 ng of DNA, including 4/5 cfDNAs (corresponding to 2 primary and 2 recurrent tumors) and 7/14 cellular DNAs (corresponding to 6 primary and 1 recurrent tumor), underwent NGS analysis together with the corresponding tumor tissues. NGS detected genetic alterations in 4/4 LP-CSF cfDNAs (corresponding to 2/32 primary and 2/6 recurrent tumors) and in 1/7 cellular DNAs (corresponding to the recurrent tumor), indicating that most cellular DNAs seem to be of non-tumor origin (Fig. 3F, Supplementary Table S10). Unlike in peritumoral cfDNA (Cohort 1), where an almost perfect match with tumor genetic alterations was found (Fig. 2I), in the case of LP-CSF cfDNA the overlapping degree was only partial, and a variable number of private alterations in either tumor or CSF were detected (Fig. 3G, Supplementary Fig. S3A-F, Supplementary Table S10 and Supplementary Data 2). These data suggest that CSF may contain subclone(s) different from those sampled in glioma tissues, well known to encompass a complex subclonal composition (35, 36).

Considering the current sensitivity limits of NGS, the low quantity of cfDNA in LP-CSF (>10 ng in only 5/38 samples) and the low rate of NGS success in cellular DNA (informative in only 1/7 cases tested), it can be concluded that attempting NGS in LP-CSF of patients with primary untreated gliomas may be debatable.

Design of LP-CSF DNA analysis by a selected panel of genetic alterations: the ITEC protocol

Next, we reasoned that: (i) cfDNA amounts found in CSF are within the sensitivity range of ddPCR, as shown by successful detection of tumor alterations in peritumoral CSF with undetectable DNA (Fig. 2E-G); (ii) a limited set of genetic alterations (*IDH1/2* mutation, p*TERT* mutations, *EGFR* amplification and *CDKN2A/2B* homozygous deletion) is currently recommended to achieve differential diagnosis between main glioma molecular subgroups, including *IDH*-wt glioblastoma on the one hand, and *IDH*-mut astrocytoma and oligodendroglioma on the other (1, 2); (iii) at least three ddPCR independent analyses should be compatible with the scanty DNA amounts recovered from LP-CSF. Indeed, the ddPCR sensitivity threshold for the above mutations is 10^{-2} ng DNA, as we measured by limiting dilution experiments (Supplementary Fig. S4A-F). Therefore, we set out to systematically analyze LP-CSF DNA (both cfDNA from supernatants and cellular DNA from pellets) by a multi-step ddPCR protocol (*IDH1*-p*TERT*-*EGFR*-*CDKN2A* protocol, hereafter named as ITEC) (Fig. 4A and B). ITEC starts with analysis of *IDH1* mutation R132H, accounting for 88.2% of overall *IDH1/2* mutations (www.cbioportal.org) and used to discriminate *IDH*-wt GBM from *IDH*-mut gliomas (1, 2). *IDH1*-mut cases are then assessed for *CDKN2A* homozygous deletion, which associates with poor prognosis and identifies grade 4 gliomas (1, 2). *IDH1*-wt DNAs

(which, in principle, may include GBM, other tumor and non-tumor DNAs) are analyzed for p*TERT* mutations (c.1-124C>T and, if negative, c.1-146C>T). As p*TERT* mutations are cumulatively expected to occur in ~90% of *IDH*-wt GBM (37), combination of *IDH1*-wt and p*TERT* mutations is highly suggestive of GBM diagnosis (Fig. 4B) (1, 2). In *IDH1*-wt and p*TERT*-wt cases, *EGFR* amplification (expected in 55% of GBM; www.cbioportal.org) is searched to support GBM diagnosis (Fig. 4B) (1, 2). We envisaged that one or more ITEC steps could fail, or that all the analyses could detect a wild-type status, leaving the diagnosis inconclusive (Fig. 4B). However, considering the frequency of the investigated genetic alterations and ddPCR assay sensitivity, we foresaw to reach a molecular diagnosis in at least 50% of cases.

LP-CSF DNA analysis by the ITEC protocol

ITEC analysis of 38 LP-CSFs showed that the first step (*IDH1* mutation) could be accomplished in 35/38 cases, while it failed in the remaining 3/38 cases, likely for insufficient DNA, leading to protocol termination (diagnosis defined as 'unfeasible', Fig. 4C, Table 1 and Supplementary Table S11). Among the above 35 samples, *IDH1* R132H mutation was detected in 1 case, followed by identification of *CDKN2A* homozygous deletion, together supporting the diagnosis of grade 4 *IDH*-mut glioma (Fig. 4C, Table 1 and Supplementary Table S11). Among *IDH1*-wt cases, 22/34 were p*TERT* mutated (either c.1-124C>T or c.1-146C>T), supporting GBM diagnosis (cases defined as 'GBM *IDH*-wt', Fig. 4C, Table 1 and Supplementary Table S11). In the remaining 12/34 cases ('*IDH*-wt undetermined'), the molecular diagnosis was not informative, because all the genetic alterations tested were wild-type (3/12 cases) or the protocol failed at the p*TERT* or *EGFR* step for DNA exhaustion (9/12 cases, Fig. 4C, Table 1 and

Supplementary Table S11). In these 12 cases, it remains undetermined whether CSF DNA was non-tumoral or related to an *IDH*-wt/p*TERT*-wt/*EGFR*-wt GBM (or to another *IDH*-wt brain tumor). Indeed, 2 LP-CSF defined as '*IDH*-wt undetermined' corresponded to GBM tumor tissues that were concomitantly *IDH*, p*TERT* and *EGFR*-wt (non-informative GBMs: MG2051, MG2056) (Fig. 4C, Table 1, Supplementary Tables S6, S7 and S11). Of note, 3 GBM cases, reported to be p*TERT*-wt by tissue analysis through Sanger sequencing, provided LP-CSF DNA where p*TERT* mutation was detected, likely as result of ddPCR higher sensitivity (MG2057, MG2062_rec and MG2064), allowing to reach the molecular diagnosis of GBM *IDH*-wt (Fig. 4C, Table 1 and Supplementary Tables S7 and S11).

Concerning the LP-CSF fraction (supernatant or cellular pellet) containing tumor DNA, in all cases but one (n = 22/23) mutations were found in cfDNA from supernatant (Table 1). Cellular DNAs from pellets were mostly wild-type, except in 4 cases (Table 1 and Supplementary Table S11). Interestingly, in 1/4 cases, tumor genetic alterations were found in cellular but not in cfDNA. These data suggest that LP-CSF cfDNA should be analyzed in the first place, but cellular DNA from pellet should not be discarded in principle.

Comparison between ITEC and standard tissue diagnosis

Molecular diagnosis reached by the ITEC protocol was consistent with histopathological and molecular diagnosis performed on tissues according to WHO 2021 guidelines (1, 2), at least as far as GBM *IDH*-wt are concerned (Fig. 4D and Table 1). The majority of cases defined as GBM *IDH*-wt by tissue histopathological and molecular diagnosis (n = 32) were either recognized (20/32), or at least defined as *IDH*-wt (11/32), while only 1/32 remained as fully undetermined (unfeasible) by ITEC (Fig. 4D and Table 1). Among tumors defined as *IDH*-mut astrocytoma or

oligodendroglioma by tissue diagnosis (n = 6), the ITEC outcome was less informative (Fig. 4D and Table 1). Beside the grade 4 *IDH*-mut astrocytoma (MG1927, see above), which was correctly identified by ITEC as a high-grade glioma, 2/6 low-grade cases failed at the first ITEC step (MG1928: grade 3 astrocytoma, MG2168: grade 2 oligodendroglioma; both defined as 'unfeasible diagnosis'; Fig. 4D and Table 1). In the remaining 3/6 cases, ITEC failed to identify *IDH1* R132H mutation: MG1943 (grade 3 *IDH*-mut astrocytoma) failed at the ensuing p*TERT* step and remained as a '*IDH*-wt undetermined', possibly because LP-CSF DNA was non-tumoral (Fig. 4D and Table 1). In two other cases (MG2064 and MG2173), ITEC reached a diagnosis inconsistent with tissue histopathological and molecular characterization. A grade 4 astrocytoma (MG2064) could not be recognized as *IDH*-mut because it was a rare case of *IDH2* rather than *IDH1* mutant, and it was identified by ITEC as GBM *IDH*-wt for the presence of p*TERT* mutation (Fig. 4C and D, Table 1 and Supplementary Table S7). Such p*TERT* mutation was not detected in the tumor tissue, where, however, *EGFR* amplification was found, leaving open the possibility that this tumor had ambiguous features; in any case, this tumor was assigned with grade 4 by histopathology (Supplementary Tables S6 and S7). The second case of inconsistency between ITEC and histopathological diagnosis was a typical 1p/19q co-deleted, *IDH1*-mut oligodendroglioma (MG2173). In this case, ITEC failed to detect *IDH1* mutation, but it detected p*TERT* mutation (found also in tissue), leading to the definition of GBM *IDH*-wt (Fig. 4D, Table 1 and Supplementary Table S7).

In summary, the ITEC protocol could be completed in 26/38 LP-CSFs, allowing to reach a molecular diagnosis in 23/26 cases. ITEC diagnosis matched integrated histological and molecular diagnosis in 21/23 cases, correctly identifying 20/32 GBM *IDH*-wt and 1/6 *IDH*-mut tumors (Fig. 4D and E and Table 1). Interestingly, within the newly diagnosed GBM group (n =

26) there was a significant correlation between shorter progression free survival (but not overall survival) on the one hand, and the possibility to reach an ITEC diagnosis, i.e. to retrieve informative DNA in LP-CSF (Fig. 4F and G, Table 1 and Supplementary Table S12). These data, together with the inconclusive ITEC results in the majority of lower grade tumors, are consistent with the notion that the presence of tumor DNA in LP-CSF is a sign of tumor aggressiveness.

Detection of *MGMT* promoter methylation in peritumoral and LP-CSF DNA

Beside genetic diagnosis, another clinically relevant marker is *MGMT* promoter methylation, which predicts response to the alkylating agent temozolomide (38). A panel of CSF cfDNAs was chosen from both Cohort 1 (n =10 primary GBM *IDH*-wt) and Cohort 2 (n = 9, including 6 primary and 2 recurrent GBM *IDH*-wt, and 1 recurrent grade 4 *IDH*-mut astrocytoma), based on sample availability after completion of respective genetic analysis protocols by ddPCR and/or NGS. CSF samples underwent *MGMT* promoter methylation analysis by beaming PCR, while matched tissues were analyzed by the same methodology in Cohort 1, or by pyrosequencing as part of routine diagnosis in Cohort 2 (Fig. 5A). In Cohort 1, this analysis revealed full concordance between peritumoral CSF and tumor DNA in 9/10 cases, while, in 1/10 cases, *MGMT* promoter methylation was detected in CSF but not in tissue (Fig. 5B and Supplementary Table S13). Also in Cohort 2 full concordance between matched tumors and LP-CSFs was observed in 8/9 cases, while in the remaining case *MGMT* promoter methylation was detected in tissue but completely absent in LP-CSF (Fig. 5C and Supplementary Table S13).

This analysis demonstrates general feasibility of *MGMT* promoter methylation detection in LP-CSF cfDNA in both recurrent and first presentation tumors. However, the DNA quantity

required for this analysis is relatively high and, considering the expected overall DNA amounts retrievable from LP-CSF, will require careful prioritization.

DISCUSSION

In patients with primary brain tumors, previous work showed that tumor DNA can be retrieved from CSF and exploited to perform comprehensive NGS, as well as more targeted analysis with high-sensitivity methodologies (16-18, 22). However, relevant questions remain open in view of systematic clinical translation of CSF-based liquid biopsy, in particular whether a broad genetic characterization is feasible in gliomas at first diagnosis. To address these issues, in the present study we analyzed two separate cohorts of newly diagnosed glioma patients, one providing peritumoral CSF collected during surgical procedures (Cohort 1), the other affording CSF by lumbar puncture immediately before surgery (Cohort 2). In both cohorts, tumor tissue and CSF genetic alterations could be systematically compared.

Consistently with previous studies (14, 16), in Cohort 1 we found that peritumoral CSF often contains relatively high cfDNA concentrations, which, through collection of a few CSF milliliters, provided DNA amounts sufficient to perform a reliable NGS analysis. However, by peritumoral cfDNA qualitative analysis, we observed previously unreported or unappreciated features, which may strongly affect tumor DNA circulation in CSF and, eventually, if and how to perform CSF liquid biopsy. In more than half peritumoral CSFs, DNA displayed, at least in part, high molecular weight (MW) while harboring tumor-specific mutations. This evidence supports that CSF DNA can often come from tumor cells that invaded liquoral spaces, or that it can be released by shedding from the surface of tumors grown up to touch such spaces. Indeed, microantomical considerations indicate that tumor DNA can transfer into CSF only minimally by ultrafiltration through the choroid plexus barrier: the latter can be crossed only by low-MW molecules (as testified by CSF physiological composition) and, unlike the brain-blood barrier, given its circumscribed localization, it is unlikely disrupted by brain tumors. Together with such

observations and considerations, our experiments, showing that glioma cells can survive in CSF for a few days and then release high-MW DNA (likely by necrosis), support a scenario in which glioma cells invading liquoral spaces release their DNA close to the tumor, where DNA can be abundantly retrieved (Fig. 6). Such DNA origin (cells actively invading CSF, or shed from tumors touching liquoral spaces) and DNA features (high-MW) greatly affect DNA circulation within CSF, and on the possibility to retrieve tumor DNA at a distance from peritumoral CSF reservoirs. Indeed, high-MW DNA is poorly soluble and thus it is expected to remain concentrated close to cells that released it (Fig. 6). Tumor cells invading liquoral spaces could in principle circulate throughout CSF, making possible their collection (or collection of DNA released by them) at a remarkable distance from their site of invasion, for example by lumbar puncture.

However, analysis of our second patient cohort indicates that cell-free tumor DNA, or intact tumor cells, are scanty in LP-CSF of newly diagnosed glioma patients, supporting a scenario where tumor DNA or cell shedding gradients rapidly fade away by departing from the tumor (Fig. 6). This is not surprising, as the low CSF pressure, and CSF circulation speed and direction are unlikely to support vigorous molecular or cellular diffusion. In our cohort, considering both LP-CSF cfDNA and cellular DNA (usually discarded in CSF liquid biopsy), 16/37 patients provided sufficient DNA (at least 10 ng) to perform NGS. However, since tumor genetic alterations were detected in all cfDNA tested, but only in a small fraction of cellular DNAs (1/7 tested), and that cfDNA retrieved from LP-CSF is usually scanty, the fraction of patients expected to provide an informative NGS result is < 20%, and even lower considering only newly diagnosed gliomas. Conversely, Miller et al. reported the presence of sufficient tumor DNA for NGS analysis in CSF cfDNA of 42/85 glioma patients who underwent LP following

clinical indications (18). However, in this study, CSF was collected long after surgery, radiotherapy and chemotherapy, when the tumor was likely progressing towards a more aggressive and invasive stage, and therapies themselves could have favored tumor cell spread to liquoral spaces.

Although in our cohort the number of LP-CSFs eligible to NGS was limited, our study was designed to provide a still missing systematic comparison between LP-CSF and tumor tissue DNA. Concordance between each tumor tissue DNA and its matched LP-CSF DNA was only partial, with several genetic alterations shared and a few alterations private either to the tumor tissue or to LP-CSF. Although the pathogenic meaning of such private alterations remains to be determined, these results suggest that LP-CSF DNA may represent only a fraction of the subclonal composition of the tumor tissue, possibly corresponding to cells endowed with greater ability to invade CSF. These findings, together with the current sensitivity limits of capture-based NGS techniques (elective to detect copy number variations, critical for glioma characterization) discourage the clinical use of LP-CSF liquid biopsy for extensive genetic characterization of diffuse gliomas at first clinical presentation.

Nonetheless, the amount of DNA retrieved from LP-CSF was within the sensitivity range of ddPCR, suggesting the possibility to analyze only the few molecular alterations essential for the differential diagnosis of adult-type diffuse glioma subgroups (in particular GBM *IDH*-wt on the one hand and *IDH*-mut astrocytomas and oligodendrogliomas on the other), according to the 2021 WHO classification of central nervous system tumors (1, 2). We therefore set up the multi-step ddPCR protocol named ITEC, sequentially analyzing *IDH*^{R132H} mutation, p*TERT* mutations, *EGFR* amplification, *CDKN2A* homozygous deletion. When at least one genetic alteration was detected (in particular *IDH1* or p*TERT* mutation), the degree of diagnostic concordance between

the ITEC protocol and the histo-molecular examination of tumor tissues was overall very satisfactory (91.3%; 21/23 cases).

The ITEC protocol performed well in recognizing *IDH*-wt GBMs (20/32 identified as *IDH*-wt/p*TERT*^{mut}), while it was less informative in the 6 cases of *IDH*-mut gliomas: in one case ITEC recognized a grade 4 *IDH*-mut recurrent glioma; in the remaining cases, ITEC failed likely for lack of tumor DNA in CSF (3 cases) or for the presence of a rare *IDH2* rather than *IDH1* mutation; only a grade 3 oligodendroglioma was misdiagnosed for a GBM *IDH*-wt, as *IDH1* mutation was not recognized and p*TERT* mutation was found. The latter case suggested the occurrence of a false negative *IDH1* R132H detection, as reported in blood-based ddPCR of *IDH*-mut advanced cholangiocarcinoma (39), but it could not rule out true negativity resulting from tumor genetic heterogeneity. Overall, in lower grade gliomas (and in part of GBMs), ITEC can be unfeasible owing to reduced aggressiveness and propensity to invade liquoral spaces, and thus to release tumor DNA in CSF. Consistently, in our exploratory analysis, newly diagnosed GBM patients that were identified by ITEC showed shorter PFS as compared with those that were not, likely because more aggressive tumors released a greater amount of tumor DNA in the CSF.

In spite of the above limitations, ITEC could split glioma patients into the two main molecular subgroups (*IDH*-wt vs. *IDH*-mut) carrying a different prognosis and therapeutic approach. Acquiring this information by a minimally invasive and overall safe (as no adverse events were registered in our cohort) LP-CSF collection might hire an extraordinary clinical significance in the management of all those cases where anatomical location or patient's comorbidities make surgical procedures challenging or simply unfeasible, or where conventional sampling methods fail to be informative. In the current formulation, the ITEC protocol does not

allow a distinction between *IDH*-mut tumors of astrocytic and oligodendroglial origin, which could be made possible by including a test assessing chromosome 1p/19q co-deletion, representing the molecular signature of oligodendrogliomas. However, in the current clinical practice, the standard post-surgical treatment for high-risk *IDH*-mut tumors, consisting of radiation followed by chemotherapy, does not differ regardless of histology. Clinicians might be helped in the differential diagnosis process by a careful revision of brain MRI including perfusion-weighted sequences, looking for typical radiological features of oligodendroglial tumors.

We can conclude that the ITEC protocol can be proposed as an alternative to broad genetic characterization for suspected gliomas not surgically approachable, at first diagnosis and during longitudinal follow-up. Although suffering from an absolute limitation such as lack of sufficient tumor DNA in LP-CSF, which could be at least in part overcome by repeating CSF collection, the protocol is flexible and amenable to introduction of tests for detection of additional or alternative genetic alterations, useful to stratify or monitor patients in much needed clinical trials.

SUPPLEMENTARY INFORMATION

Supplementary Information includes: Supplementary Figures 1-4, Supplementary Tables S1-S13, Supplementary Materials and Methods, Supplementary References. Supplementary Files include Supplementary Data 1-3.

AUTHORS' CONTRIBUTIONS

F. Orzan: Conceptualization, data curation, formal analysis, validation, investigation, visualization, methodology, writing-original draft, writing-review and editing. **F. De Bacco:** Conceptualization, data curation, formal analysis, validation, investigation, visualization, writing-original draft, writing-review and editing. **E. Lazzarini:** Data curation, formal analysis, investigation. **G. Crisafulli:** Data curation, formal analysis, validation. **A. Gasparini:** Data curation, investigation, methodology. **A. Dipasquale:** Resources, data curation, writing-original draft, writing-review and editing. **L. Barault:** Data curation, investigation, methodology. **M. Macagno:** Data curation, investigation. **P. Persico:** Resources. **F. Pessina:** Resources. **B. Bono:** Resources. **L. Giordano:** Formal analysis. **P. Zeppa:** Resources, data curation. **A. Melcarne:** Resources. **P. Cassoni:** Resources. **D. Garbossa:** Resources, supervision. **A. Santoro:** Resources, supervision. **P. M. Comoglio:** Supervision, funding acquisition. **S. Indraccolo:** Data curation, supervision, funding acquisition, methodology, project administration. **M. Simonelli:** Conceptualization, resources, data curation, supervision, funding acquisition, writing-original draft, project administration, writing-review and editing. **C. Boccaccio:** Conceptualization, data curation, supervision, funding acquisition, visualization, writing-original draft, project administration, writing-review and editing.

ACKNOWLEDGMENTS

Schemes (Fig. 1A, Fig. 3A, Fig. 4A, Fig. 5A and Fig. 6) were created with Biorender.com.

We thank F. Di Nicolantonio for discussion, R. Altieri for help with patients' management, G. Reato, E. Casanova, M. Prelli, A. Bartolini, B. Mussolin, B. Martinoglio, R. Porporato, S. Gilardi, V. Pessei, L. Pasqualini, for technical help.

This work was supported by AIRC - Italian Association for Cancer Research Investigator Grant N. 19933 to C. Boccaccio and N. 23820 to P. M. Comoglio; Comitato per Albi98 to C. Boccaccio; Italian Ministry of Health RC 2022 to C. Boccaccio; IOV intramural research grant 2017 – 5 × 1000 (MAGIC-2) to S. Indraccolo; Italian Ministry of Health, Alleanza Contro il Cancro (ACC) Network Project RCR-2021-23671213 to S. Indraccolo, C. Boccaccio and M. Simonelli.

REFERENCES

1. Louis DN, Perry A, Wesseling P, Brat DJ, Cree IA, Figarella-Branger D, et al. The 2021 WHO Classification of Tumors of the Central Nervous System: a summary. Neuro Oncol 2021;23:1231-51.

2. Weller M, van den Bent M, Preusser M, Le Rhun E, Tonn JC, Minniti G, et al. EANO guidelines on the diagnosis and treatment of diffuse gliomas of adulthood. Nat Rev Clin Oncol 2021;18:170-86.

3. Wen PY, Packer RJ. The 2021 WHO Classification of Tumors of the Central Nervous System: clinical implications. Neuro Oncol 2021;23:1215-7.

4. Chakravarty D, Solit DB. Clinical cancer genomic profiling. Nat Rev Genet 2021;22:483-501.

5. Nicholson JG, Fine HA. Diffuse Glioma Heterogeneity and Its Therapeutic Implications. Cancer Discov 2021;11:575-90.

6. Simonelli M, Dipasquale A, Orzan F, Lorenzi E, Persico P, Navarria P, et al. Cerebrospinal fluid tumor DNA for liquid biopsy in glioma patients' management: Close to the clinic? Crit Rev Oncol Hematol 2020;146:102879.

7. Escudero L, Martínez-Ricarte F, Seoane J. ctDNA-Based Liquid Biopsy of Cerebrospinal Fluid in Brain Cancer. Cancers (Basel). 2021;13:1989.

8. Soffietti R, Bettegowda C, Mellinghoff IK, Warren KE, Ahluwalia MS, De Groot JF, et al. Liquid biopsy in gliomas: a RANO review and proposals for clinical applications. Neuro Oncol 2022;24:855-71.

9. Mellinghoff IK, Ellingson BM, Touat M, Maher E, De La Fuente MI, Holdhoff M, et al. Ivosidenib in Isocitrate Dehydrogenase 1. J Clin Oncol 2020;38:3398-406.

10. Wen PY, Stein A, van den Bent M, De Greve J, Wick A, de Vos FYFL, et al. Dabrafenib plus trametinib in patients with BRAF. Lancet Oncol 2022;23:53-64.

11. Doz F, van Tilburg CM, Geoerger B, Højgaard M, Øra I, Boni V, et al. Efficacy and safety of larotrectinib in TRK fusion-positive primary central nervous system tumors. Neuro Oncol 2022;24:997-1007.

12. Meric-Bernstam F, Bahleda R, Hierro C, Sanson M, Bridgewater J, Arkenau HT, et al. Futibatinib, an Irreversible FGFR1-4 Inhibitor, in Patients with Advanced Solid Tumors Harboring. Cancer Discov 2022;12:402-15.

13. Le Fèvre C, Constans JM, Chambrelant I, Antoni D, Bund C, Leroy-Freschini B, et al. Pseudoprogression versus true progression in glioblastoma patients: A multiapproach literature review. Part 2 - Radiological features and metric markers. Crit Rev Oncol Hematol 2021;159:103230.

14. Bettegowda C, Sausen M, Leary RJ, Kinde I, Wang Y, Agrawal N, et al. Detection of circulating tumor DNA in early- and late-stage human malignancies. Sci Transl Med 2014;6:224ra24.

15. Wang Y, Springer S, Zhang M, McMahon KW, Kinde I, Dobbyn L, et al. Detection of tumor-derived DNA in cerebrospinal fluid of patients with primary tumors of the brain and spinal cord. Proc National Acad Sci U S A 2015;112:9704-9.

16. De Mattos-Arruda L, Mayor R, Ng CKY, Weigelt B, Martínez-Ricarte F, Torrejon D, et al. Cerebrospinal fluid-derived circulating tumour DNA better represents the genomic alterations of brain tumours than plasma. Nat Commun 2015;6:8839.

17. Pentsova EI, Shah RH, Tang J, Boire A, You D, Briggs S, et al. Evaluating Cancer of the Central Nervous System Through Next-Generation Sequencing of Cerebrospinal Fluid. J Clin Oncol 2016;34:2404-15.

18. Miller AM, Shah RH, Pentsova EI, Pourmaleki M, Briggs S, Distefano N, et al. Tracking tumour evolution in glioma through liquid biopsies of cerebrospinal fluid. Nature 2019;565:654-8.

19. Mouliere F, Mair R, Chandrananda D, Marass F, Smith CG, Su J, et al. Detection of cell-free DNA fragmentation and copy number alterations in cerebrospinal fluid from glioma patients. EMBO Mol Med 2018;10:e9323.

20. Juratli TA, Stasik S, Zolal A, Schuster C, Richter S, Daubner D, et al. Promoter Mutation Detection in Cell-Free Tumor-Derived DNA in Patients with. Clin Cancer Res 2018;24:5282-91.

21. Huang TY, Piunti A, Lulla RR, Qi J, Horbinski CM, Tomita T, et al. Detection of Histone H3 mutations in cerebrospinal fluid-derived tumor DNA from children with diffuse midline glioma. Acta Neuropathol Commun 2017;5:28.

22. Martínez-Ricarte F, Mayor R, Martínez-Sáez E, Rubio-Pérez C, Pineda E, Cordero E, et al. Molecular Diagnosis of Diffuse Gliomas through Sequencing of Cell-Free Circulating Tumor DNA from Cerebrospinal Fluid. Clin Cancer Res 2018;24:2812-9.

23. Escudero L, Llort A, Arias A, Diaz-Navarro A, Martínez-Ricarte F, Rubio-Perez C, et al. Circulating tumour DNA from the cerebrospinal fluid allows the characterisation and monitoring of medulloblastoma. Nat Commun 2020;11:5376.

24. Steinhaus R, Proft S, Schuelke M, Cooper DN, Schwarz JM, Seelow D. MutationTaster2021. Nucleic Acids Res 2021;49:W446-51.

25. de Andrade KC, Lee EE, Tookmanian EM, Kesserwan CA, Manfredi JJ, Hatton JN, et al. The TP53 Database: transition from the International Agency for Research on Cancer to the US National Cancer Institute. Cell Death Differ 2022;29:1071-3.

26. Corless BC, Chang GA, Cooper S, Syeda MM, Shao Y, Osman I, et al. Development of Novel Mutation-Specific Droplet Digital PCR Assays Detecting TERT Promoter Mutations in Tumor and Plasma Samples. J Mol Diagn 2019;21:274-85.

27. Eng J. Sample size estimation: how many individuals should be studied? Radiology 2003;227:309-13.

28. Lombardi G, Barresi V, Indraccolo S, Simbolo M, Fassan M, Mandruzzato S, et al. Pembrolizumab Activity in Recurrent High-Grade Gliomas with Partial or Complete Loss of Mismatch Repair Protein Expression: A Monocentric, Observational and Prospective Pilot Study. Cancers (Basel) 2020;12:2283.

29. Corti G, Bartolini A, Crisafulli G, Novara L, Rospo G, Montone M, et al. A Genomic Analysis Workflow for Colorectal Cancer Precision Oncology. Clin Colorectal Cancer 2019;18:91-101.e3.

30. Crisafulli G, Mussolin B, Cassingena A, Montone M, Bartolini A, Barault L, et al. Whole exome sequencing analysis of urine trans-renal tumour DNA in metastatic colorectal cancer patients. ESMO Open. 2019;4:e000572.

31. Crisafulli G, Sartore-Bianchi A, Lazzari L, Pietrantonio F, Amatu A, Macagno M, et al. Temozolomide Treatment Alters Mismatch Repair and Boosts Mutational Burden in Tumor and Blood of Colorectal Cancer Patients. Cancer Discov 2022;12:1656-75.

32. Chakravarty D, Gao J, Phillips SM, Kundra R, Zhang H, Wang J, et al. OncoKB: A Precision Oncology Knowledge Base. JCO Precis Oncol 2017; 2017:PO.17.00011.

33. Li M, Chen WD, Papadopoulos N, Goodman SN, Bjerregaard NC, Laurberg S, et al. Sensitive digital quantification of DNA methylation in clinical samples. Nat Biotechnol 2009;27:858-63.

34. Wan JCM, Massie C, Garcia-Corbacho J, Mouliere F, Brenton JD, Caldas C, et al. Liquid biopsies come of age: towards implementation of circulating tumour DNA. Nat Rev Cancer 2017;17:223-38.

35. Sottoriva A, Spiteri I, Piccirillo SG, Touloumis A, Collins VP, Marioni JC, et al. Intratumor heterogeneity in human glioblastoma reflects cancer evolutionary dynamics. Proc National Acad Sci U S A 2013;110:4009-14.

36. Kim J, Lee IH, Cho HJ, Park CK, Jung YS, Kim Y, et al. Spatiotemporal Evolution of the Primary Glioblastoma Genome. Cancer Cell 2015;28:318-28.

37. Barthel FP, Wei W, Tang M, Martinez-Ledesma E, Hu X, Amin SB, et al. Systematic analysis of telomere length and somatic alterations in 31 cancer types. Nat Genet 2017;49:349-57.

38. Reifenberger G, Wirsching HG, Knobbe-Thomsen CB, Weller M. Advances in the molecular genetics of gliomas - implications for classification and therapy. Nat Rev Clin Oncol 2017;14:434-52.

39. Lapin M, Huang HJ, Chagani S, Javle M, Shroff RT, Pant S, et al. Monitoring of Dynamic Changes and Clonal Evolution in Circulating Tumor DNA From Patients With. JCO Precis Oncol 2022;6:e2100197.

FIGURE LEGENDS

Figure 1.

Cohort 1: experimental design for glioma and CSF comparative analysis, and tumor characterization **A,** Experimental design. Cohort 1 patients provided fresh tumor tissues (*n* = 45), CSF sampled from liquoral spaces in proximity with the surgical field (peritumoral CSF, *n* = 45) and blood samples (*n* = 42). Tumor tissue DNA underwent analysis of frequently occurring glioma genetic alterations (by Sanger sequencing and qPCR, step 1). Genetic alterations of informative tumors were searched in cell-free DNA (cfDNA) isolated from CSF or blood plasma by ddPCR assays tailored on the specific sequence alterations (step 2). Selected tumor tissue and CSF DNA samples underwent NGS (step 3). **B,** Glioma histopathological and molecular diagnosis, and genetic alterations in a selected panel of GBM-associated genes, detected by Sanger sequencing (mutations) and qPCR analysis (copy number variations) in tumor tissues.

Figure 2.

Cohort 1: comparative analysis of peritumoral CSF and tumor tissues **A,** Analysis of DNA amount vs. CSF volume in peritumoral CSF samples from Cohort 1 (*n* = 45). Red line indicates the threshold of minimal DNA content (10 ng) for NGS analysis (Spearman correlation between total CSF DNA amount and volume, $r = 0.36$, $p = 0.014$). **B,** Analysis of cfDNA concentration in peritumoral CSF samples from Cohort 1 (*n* = 45). Grey line: median DNA concentration = 77.2 ng/ml. **C,** Correlation between peritumoral CSF cfDNA concentration and tumor features such as proximity to a CSF space (ventricle or cistern), tumor grade and size. Median cfDNA concentrations were compared between groups defined by proximity to CSF space or tumor grades (non parametric Wilcoxon-Mann-Whitney test). Maximal tumor diameter and areas (as

reported in Supplementary Table S1) were correlated with cfDNA concentration in all CSF samples (Pearson correlation). n: number of tumors. **D,** cfDNA analysis showing the presence of either low (L) or high (H) or mixed (MIX) molecular weight (MW) DNA in representative CSF samples (Bioanalyzer output). **E** and **F,** Heatmaps showing peritumoral CSF samples eligible to ddPCR (n = 36) analyzed for selected genetic alterations found in the corresponding tumors. (**E**) copy number variations (CNV). Red: amplifications (CN > 5) and gains (3 < CN < 5); blue: deletions (CN < 1.5). Color legend for CNV is shown. (**F**) gene mutations. Color legend for VAF (variant allele frequency) is shown. VAF < 10% are reported. *: samples tested for both CNV and mutations. **G,** Dot plot indicating cfDNA concentration and MW features in the groups of peritumoral CSF samples where tumor genetic alterations were detected (yes) or not (no) by ddPCR. No statistically significant association was found between DNA MW type and the possibility to detect mutations in CSF (Chi-square test for a trend, P = 0.39, df = 1). **H,** Flow-chart: shortlisting of peritumoral CSF samples from sample collection to eligibility to NGS analysis. **I,** Comparative NGS analysis showing correspondence between matched peritumoral CSF cfDNAs and tumor tissue DNAs. CSF cfDNA total amount, concentration and quality (MW), and VAF < 10% are reported. Color legends for heatmaps (CN and VAF) are shown.

Figure 3.

Cohort 2: LP-CSF NGS analysis **A,** Experimental design. Cohort 2 patients yielded fresh or archive tumor tissues (n = 40) and CSF sampled by LP (LP-CSF, n = 40). From LP-CSF, DNA was recovered from either the supernatant (cfDNA) or the pellet (cellular DNA). Wherever possible, tumor tissue DNA and LP-CSF DNA were compared by NGS analysis. **B,** Oncoprint of Cohort 2 patients based on detection of *IDH1*/2 mutation by IHC, p*TERT* sequencing, and *EGFR*

amplification analysis by FISH. **C,** Analysis of DNA concentration in LP-CSF samples (cfDNA from supernatants or cellular DNA from pellets) in Cohort 2. Grey line: median DNA concentration (cfDNA = 0.05 ng/ml; cellular DNA = 2.14 ng/ml). **D,** Analysis of DNA amount (cfDNA from supernatants and cellular DNA from pellets) vs. LP-CSF volume in samples from Cohort 2 (n = 38). Primary or recurrent tumors are indicated. Red line indicates the threshold of minimal DNA content (10 ng) required for NGS analysis (Spearman correlation between cfDNA amount and LP-CSF volume, r = 0.38, p = 0.021; between cellular DNA and LP-CSF volume, r = 0.10, p =0.56). **E,** Correlation between tumor features (proximity to CSF space, tumor grade and size) on the one hand, and LP-CSF cfDNA concentration on the other. Median DNA concentrations were compared between groups defined by proximity to CSF space or tumor grades (non parametric Wilcoxon-Mann-Whitney test). Maximal tumor diameter and areas (as reported in Supplementary Table S9) were correlated with DNA concentration in LP-CSF samples (Pearson correlation). n: number of tumors Red: statistically significant correlation. **F,** Flow-chart: shortlisting of LP-CSF samples from collection to NGS eligibility and overall results. **G,** Venn diagrams summarizing NGS results, showing the degree of correspondence between paired LP-CSF (cfDNA or cellular DNA) and tumor tissue DNA. Pairing between tumor and LP-CSF was verified by SNP ID (Supplementary Data 3). Bold: single nucleotide variations. Regular: copy number variations.

Figure 4.

Cohort 2: targeted analysis of LP-CSF for glioma differential diagnosis **A,** Experimental design. In Cohort 2 glioma patients, DNA recovered from LP-CSF (n = 38), either from supernatant (cfDNA, n = 38) or pellet (cellular DNA, n = 35), underwent the ITEC protocol. **B,** Schematic

of ITEC protocol. **C,** Oncoprint of genetic alterations detected through the ITEC protocol and the resulting diagnosis according to WHO 2021 definitions. *IDH*-wt undetermined: GBM or other tumor type or non-tumoral DNA; unfeasible: ITEC protocol stopped at first step. **D,** Graph showing concordance (grey bars) between diagnosis based on histopathological and molecular criteria (according to WHO2021) and ITEC-based molecular diagnosis. **E,** Flowchart: sample shortlisting from LP-CSF sample collection to ITEC protocol outcome. **F** and **G,** Correlation between attainment of ITEC diagnosis and progression free survival (PFS, significant, **F**) and overall survival of primary GBM patients (not significant but in the same trend, **G**).

Figure 5.

Cohort 1 and 2: *MGMT* promoter methylation in peritumoral and LP-CSF cfDNA **A**, Experimental design. A panel of matched tumor tissues and CSFs (Cohort 1: n = 10; Cohort 2: n = 9) underwent evaluation of *MGMT* promoter methylation either by beaming PCR or pyrosequencing. **B,** Cohort 1, percentage of *MGMT* promoter methylation measured by beaming PCR in a panel of matched tumor DNAs and peritumoral CSF cfDNAs. **C,** Cohort 2, percentage of *MGMT* promoter methylation measured in a panel of matched tumor DNAs (pyrosequencing) and LP-CSF cfDNAs (beaming PCR). Dotted line: threshold to define *MGMT* promoter methylation (30%).

Figure 6.

Features and origins of DNA found in CSF. Evidence provided in this study supports that brain tumor DNA found in CSF mostly derives from tumor cells invading liquoral spaces (or shed from tumors touching liquoral spaces), which can release both high- and low-molecular weight

(MW) DNA as result of necrosis and/or apoptosis, respectively. A small amount of low-MW DNA is expected to be secreted into CSF by ultrafiltration at the physiological site of CSF formation (choroid plexus). High-MW DNA is poorly soluble and minimally diffuses throughout CSF. Low-MW DNA is soluble, but the slow dynamic of CSF circulation can prevent its diffusion from the site of cell invasion to the distant point of CSF collection (lumbar puncture).

Table 1. Cohort 2, ITEC protocol results (ddPCR).

Sample ID	IDH1	pTERT[(1)]	pTERT[(2)]	EGFR	CDKN2A	Histopath./mol diagnosis (WHO 2021)	ITEC diagnosis	Matched diagnosis	DNA type
MG1926	failed	n.a.	n.a.	n.a.	n.a.	GBM IDH-wt	unfeasible	n.d.	cfDNA
MG1927_rec	mut	-	-	-	del	grade 4 IDH-mut astrocytoma	grade 4 IDH-mut astrocytoma	yes	cfDNA
MG1928	failed	n.a.	n.a.	n.a.	n.a.	grade 3 IDH-mut astrocytoma	unfeasible	n.d.	cfDNA
MG1938	wt	mut	-	-	-	GBM IDH-wt	GBM IDH-wt	yes	cfDNA
MG1942_rec	wt	mut	-	-	-	GBM IDH-wt	GBM IDH-wt	yes	cfDNA
MG1943	wt[a]	failed	n.a.	n.a.	-	grade 3 IDH-mut astrocytoma	IDH-wt undetermined	no	cfDNA
MG1944	wt	failed	n.a.	n.a.	-	GBM IDH-wt	IDH-wt undetermined	n.d.	cfDNA
MG1945	wt	mut	-	-	-	GBM IDH-wt	GBM IDH-wt	yes	cfDNA
MG2046	wt	mut	-	-	-	GBM IDH-wt	GBM IDH-wt	yes	cfDNA
MG2047	wt	wt	wt	failed	-	GBM IDH-wt	IDH-wt undetermined	n.d.	cfDNA
MG2048	wt	mut	-	-	-	GBM IDH-wt	GBM IDH-wt	yes	both
MG2049	wt	wt	failed	n.a.	-	GBM IDH-wt	IDH-wt undetermined	n.d.	cfDNA
MG2049_rec	wt	mut	-	-	-	GBM IDH-wt	GBM IDH-wt	yes	cfDNA
MG2050	wt	wt	mut	-	-	GBM IDH-wt	GBM IDH-wt	yes	cfDNA
MG2051[b]	wt	wt	wt	wt	-	GBM IDH-wt	IDH-wt undetermined	n.d.	cfDNA
MG2052	wt	wt	failed	n.a.	-	GBM IDH-wt	IDH-wt undetermined	n.d.	cfDNA
MG2053	wt	mut	-	-	-	GBM IDH-wt	GBM IDH-wt	yes	cfDNA
MG2054	wt	wt	mut	-	-	GBM IDH-wt	GBM IDH-wt	yes	cfDNA
MG2055_rec	wt	failed	n.a.	n.a.	-	GBM IDH-wt	IDH-wt undetermined	n.d.	cfDNA
MG2056[b]	wt	wt	wt	wt	-	GBM IDH-wt	IDH-wt undetermined	n.d.	cfDNA
MG2057[b]	wt	mut[a]	-	-	-	GBM IDH-wt	GBM IDH-wt	yes	cfDNA
MG2058_rec	wt	failed	n.a.	n.a.	-	GBM IDH-wt	IDH-wt undetermined	n.d.	cfDNA
MG2059	wt	failed	n.a.	n.a.	-	GBM IDH-wt	IDH-wt undetermined	n.d.	cfDNA
MG2060	wt	failed	n.a.	n.a.	-	GBM IDH-wt	IDH-wt undetermined	n.d.	cfDNA
MG2061	wt	mut	-	-	-	GBM IDH-wt	GBM IDH-wt	yes	cfDNA
MG2062_rec[b]	wt	mut[a]	-	-	-	GBM IDH-wt	GBM IDH-wt	yes	cfDNA
MG2063	wt	mut	-	-	-	GBM IDH-wt	GBM IDH-wt	yes	cfDNA
MG2064[b]	wt	mut[a]	-	-	-	grade 4 IDH2-mut astrocytoma	GBM-IDH wt	no	cfDNA
MG2065	wt	mut	-	-	-	GBM IDH-wt	GBM IDH-wt	yes	cfDNA
MG2166	wt	mut	-	-	-	GBM IDH-wt	GBM IDH-wt	yes	both
MG2168	failed	n.a.	n.a.	n.a.	n.a.	grade 2 IDH-mut oligodendroglioma	unfeasible	n.d.	cfDNA
MG2169	wt	mut	-	-	-	GBM IDH-wt	GBM IDH-wt	yes	cfDNA
MG2170	wt	mut	-	-	-	GBM IDH-wt	GBM IDH-wt	yes	both
MG2171	wt	wt	wt	wt	-	GBM IDH-wt	IDH-wt undetermined	n.d.	cfDNA
MG2172	wt	mut	-	-	-	GBM IDH-wt	GBM IDH-wt	yes	cfDNA
MG2173	wt[a]	mut[c]	-	-	-	grade 3 IDH-mut oligodendroglioma	GBM IDH-wt	no	cellDNA
MG2177	wt	mut	-	-	-	GBM IDH-wt	GBM IDH-wt	yes	cfDNA
MG2179	wt	mut	-	-	-	GBM IDH-wt	GBM IDH-wt	yes	cfDNA

[1]: pTERT mutation c.1-124C>T.
[2]: pTERT mutation c.1-146C>T.
[a]: CSF discordant from tissue molecular diagnosis (Supplementary Table S7).
[b]: IDH1-wt and pTERT-wt "non-informative" tumors (Supplementary Table S7).
[c]: pTERT mutation detected only in CSF cellular DNA.
n.a.: not assessed, after failure of IDH1 or pTERT analysis.
-: not assessed, after protocol termination.
n.d.: not determined.

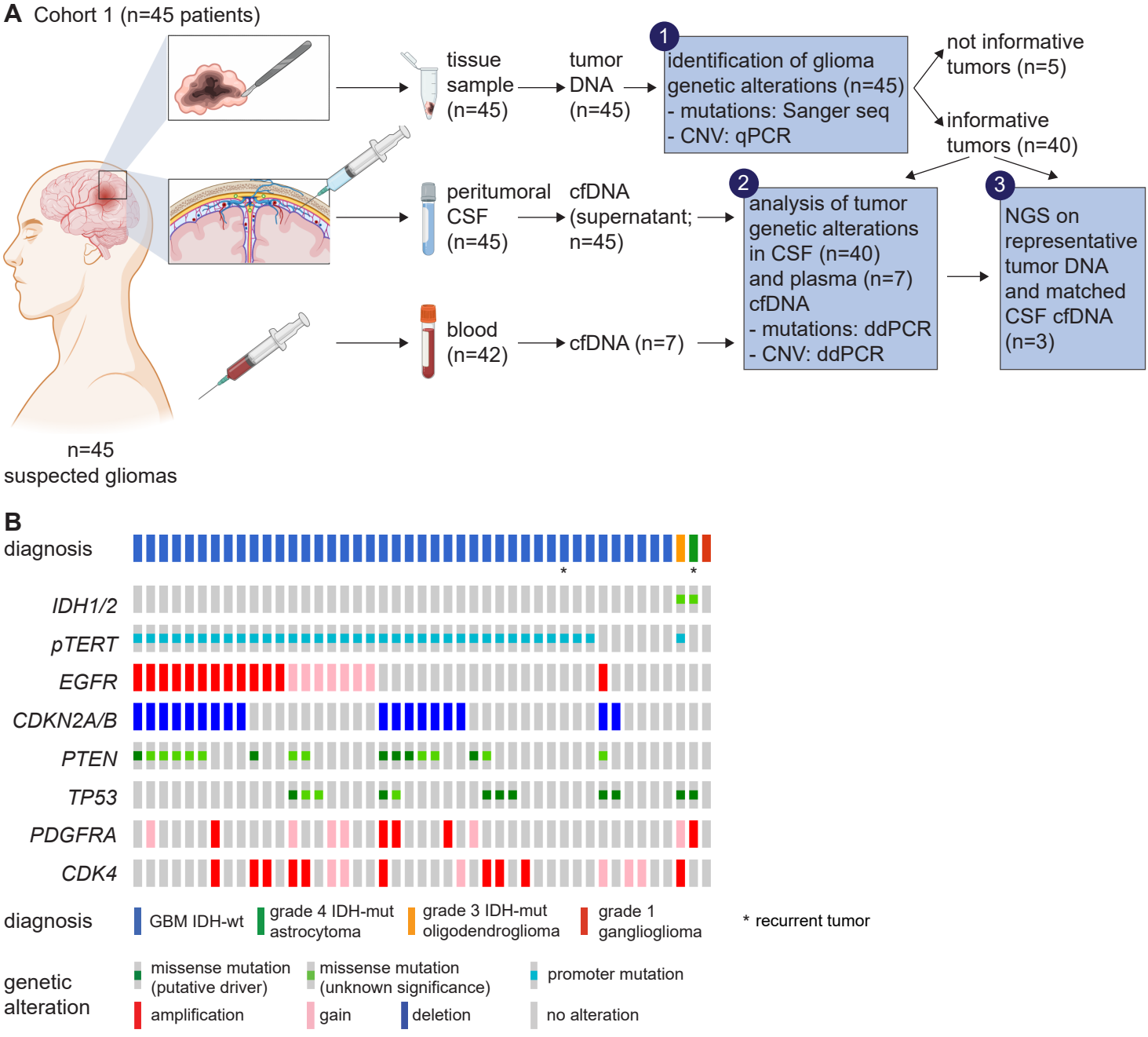

Figure 1

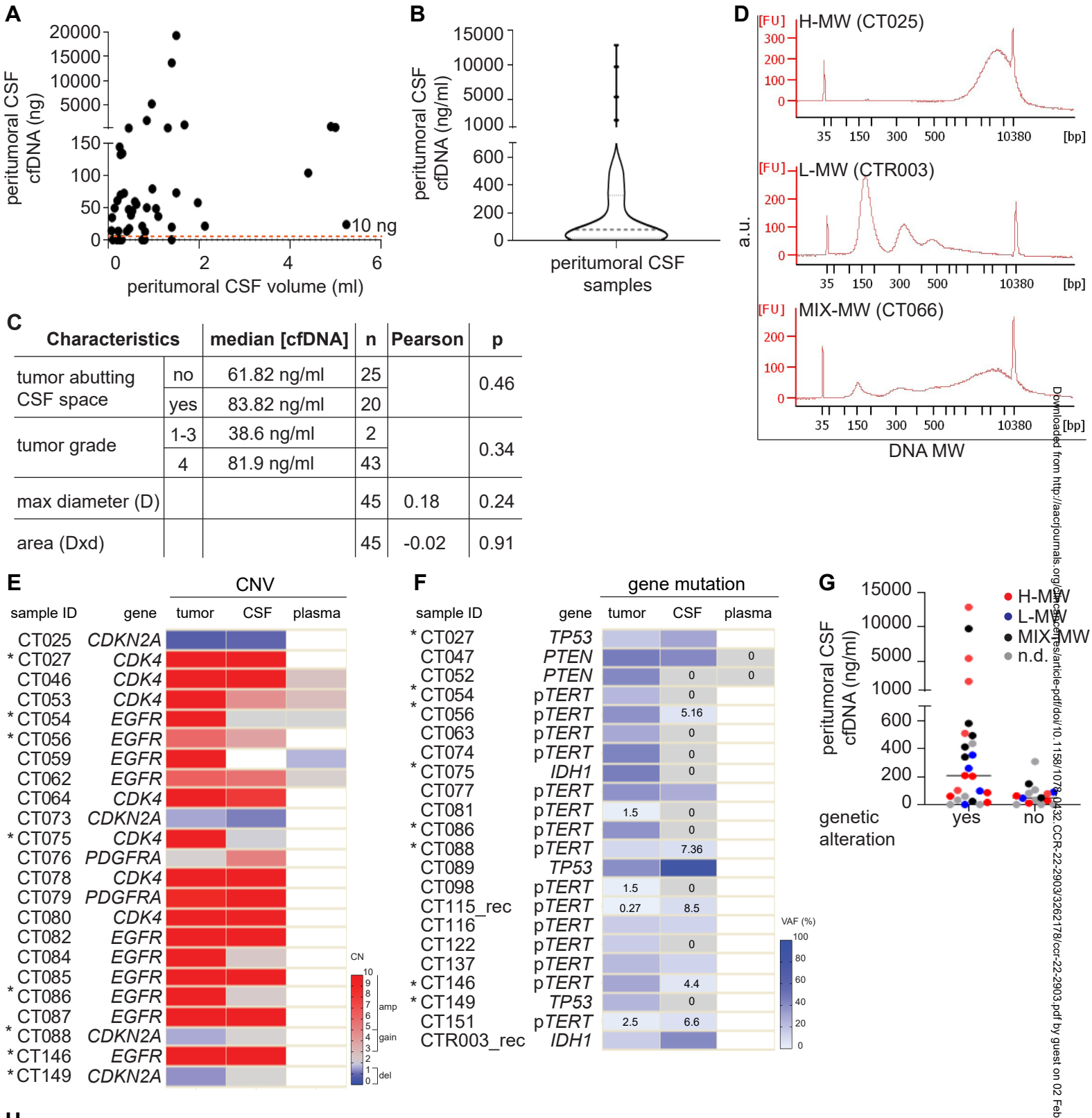

C

Characteristics		median [cfDNA]	n	Pearson	p
tumor abutting CSF space	no	61.82 ng/ml	25		0.46
	yes	83.82 ng/ml	20		
tumor grade	1-3	38.6 ng/ml	2		0.34
	4	81.9 ng/ml	43		
max diameter (D)			45	0.18	0.24
area (Dxd)			45	-0.02	0.91

H

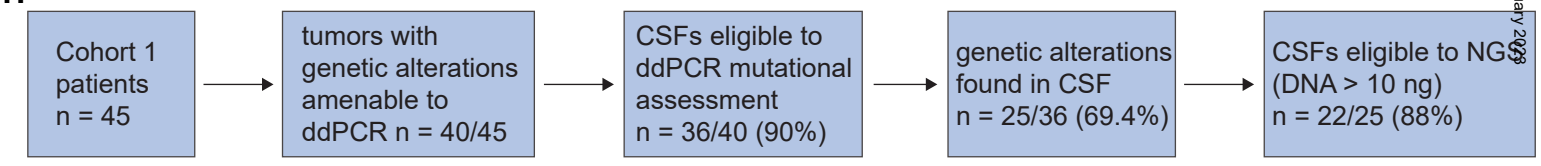

I

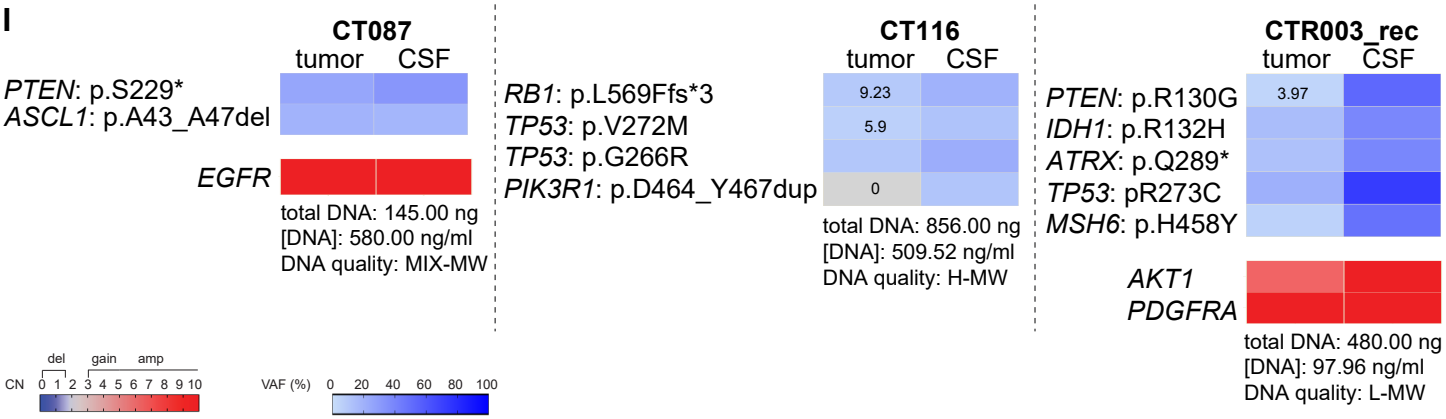

Figure 2

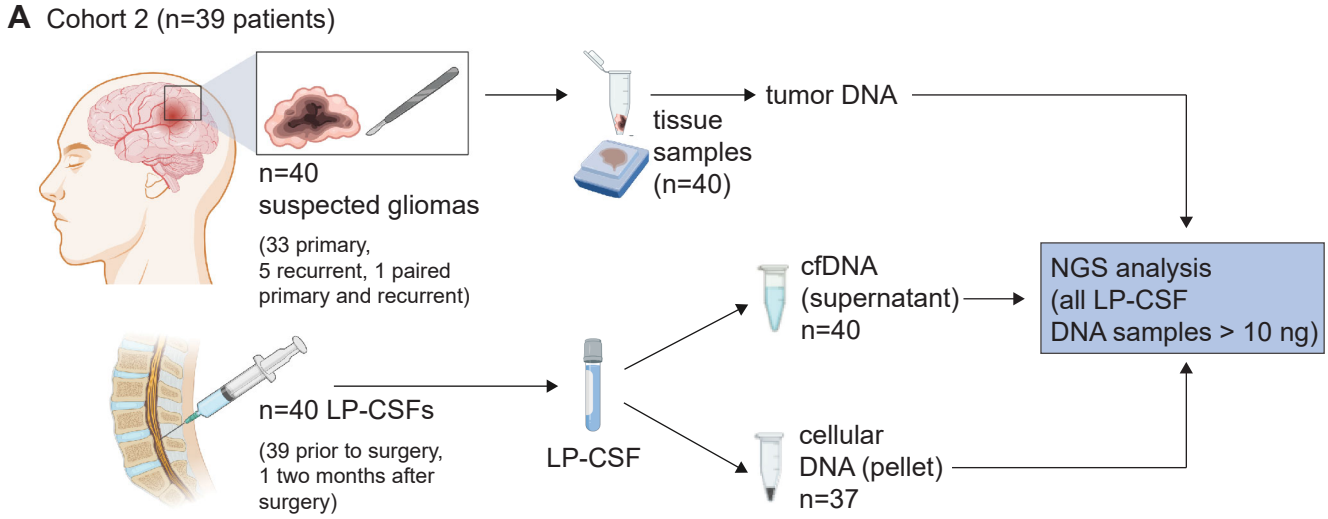

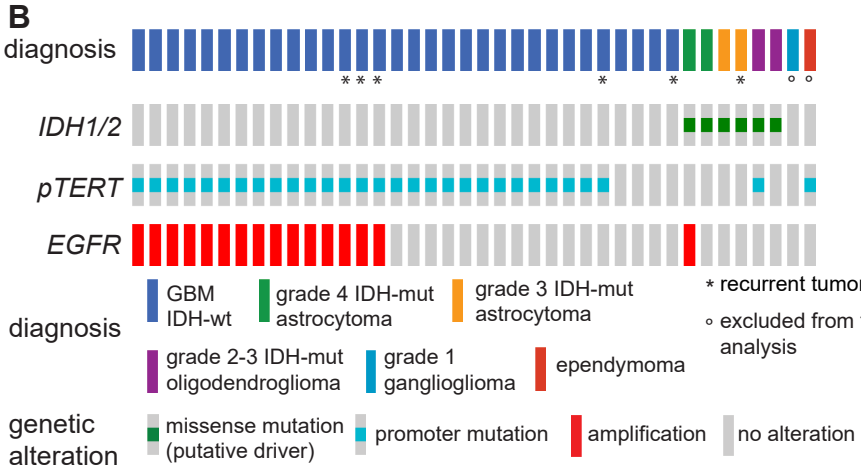

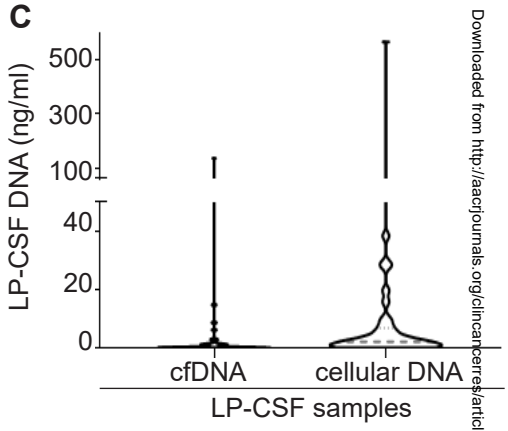

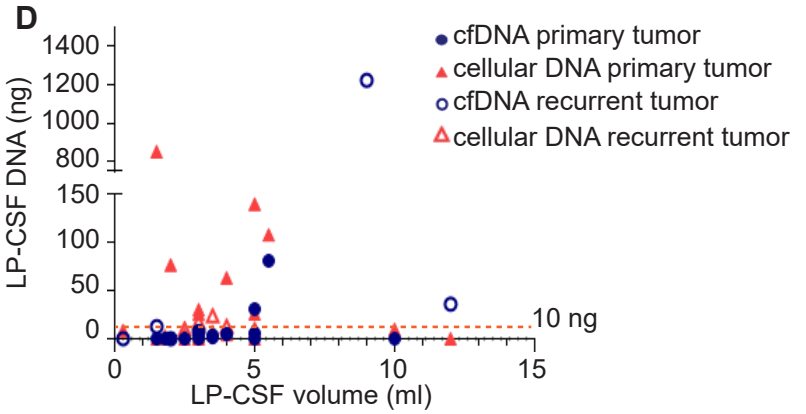

E

Characteristics		median [cfDNA]	n	Pearson	p
tumor abutting CSF space	no	0.033 ng/ml	18		0.03
	yes	0.39 ng/ml	20		
tumor grade	1-3	0.04 ng/ml	4		0.51
	4	0.053 ng/ml	34		
max diameter (D)			37	0.22	0.19
area (Dxd)			37	0.15	0.36

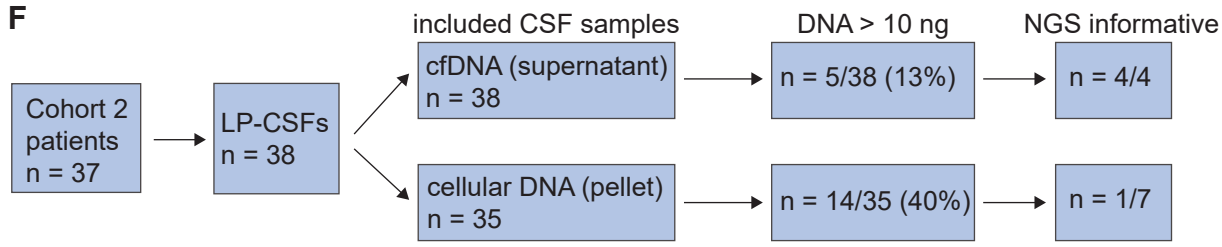

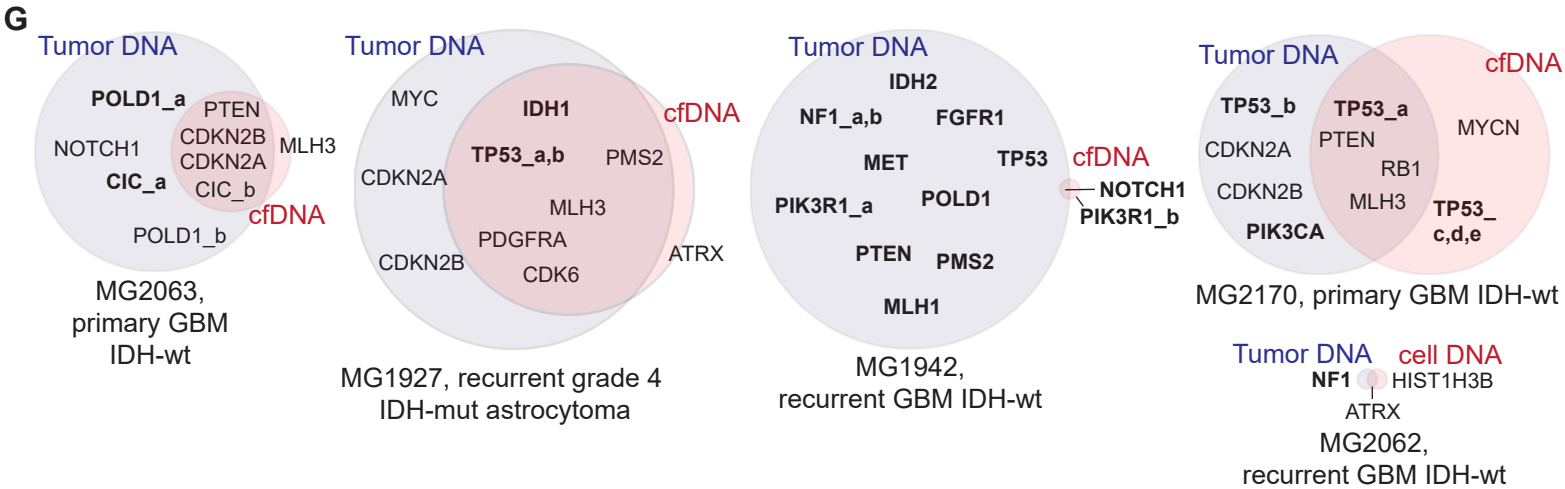

Figure 3

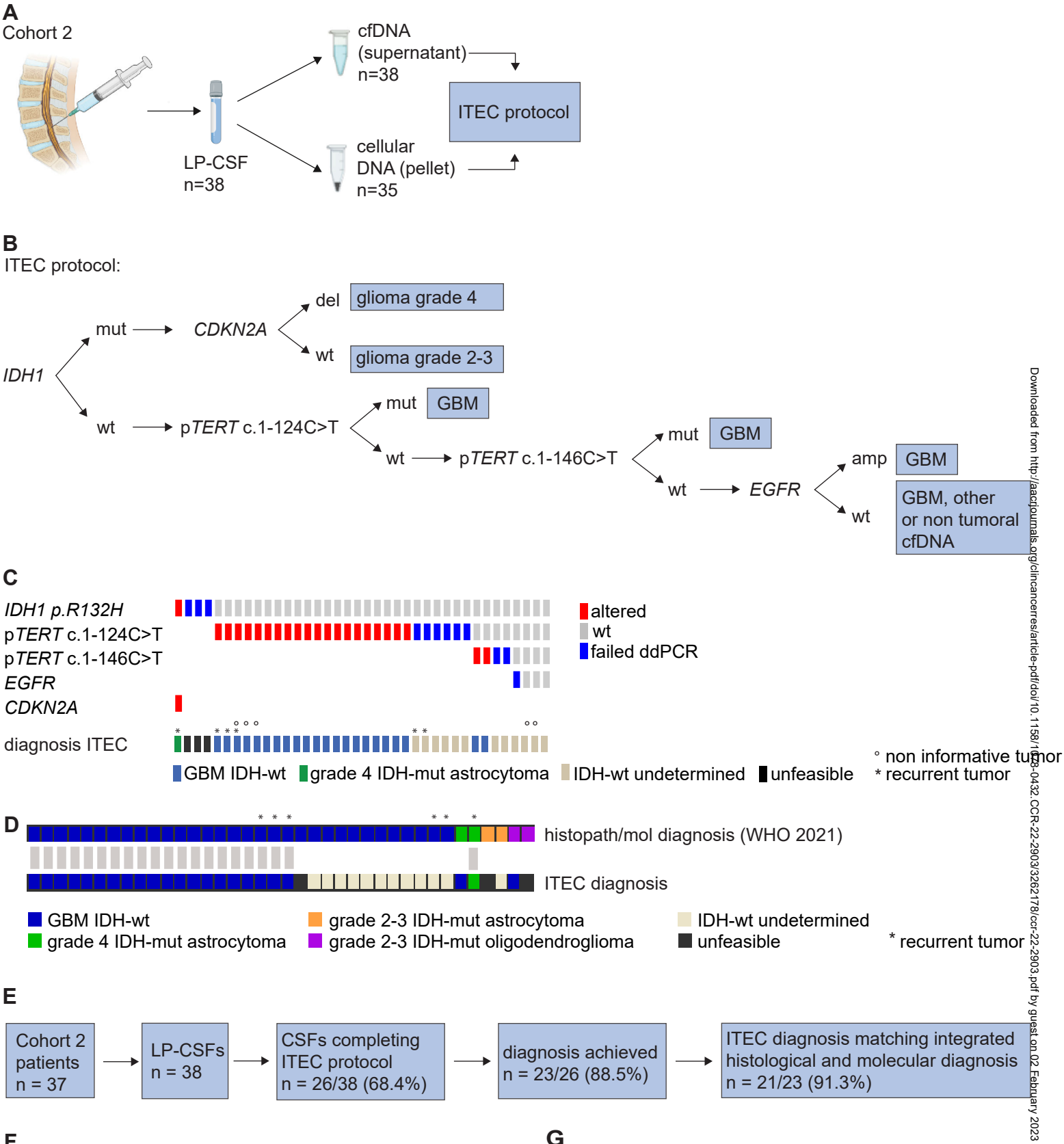

Figure 4

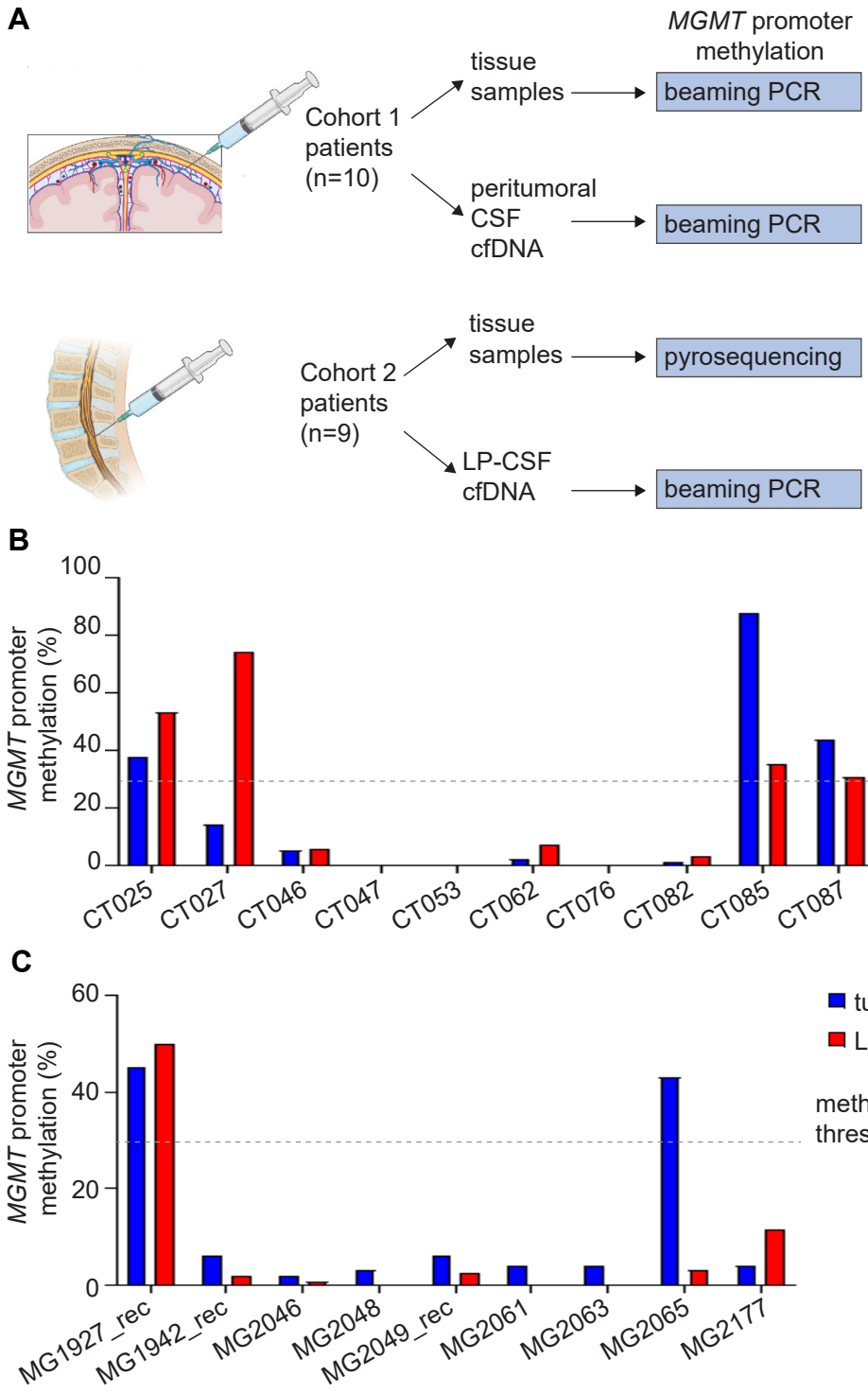

Figure 5

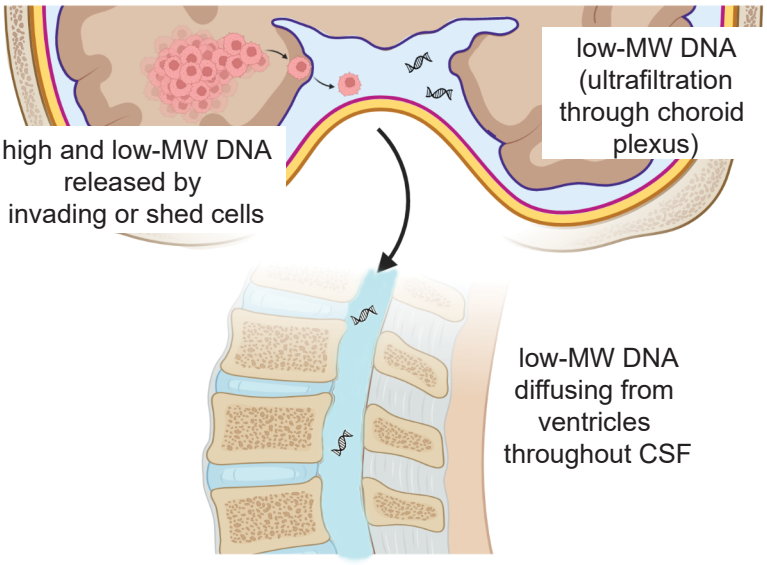

Figure 6